MEASUREMENT OF THERMAL STRESS AND PREDICTION OF FATIGUE FOR STS USING LOCK-IN THERMOGRAPHY

Won-Tae Kim[1+], Dr Man-Yong Choi[2], Dr. Yong-Hak Huh[2], Sung-Jin Eom[3]

[1]Kongju National University, Chungnam, Korea
[2]Korea Research Institute of Standards and Science, Daejeon, Korea
[3]HanMac Corp., Seoul, Korea

Abstract

This paper aims to describe the thermal stress analysis and fatigue-limit prediction using Lock-in thermography as a nondestructive testing (NDT) method with real time. Due to the first and second principles of thermodynamics, there is a relationship between temperature and mechanical behavior laws. Applying the IR thermography measurement to standard tensile specimen (STS) with diverse notches machined artificially, thermal stress is measured under several dynamic loading conditions excited from external disturbances. Since fatigue testing would significantly reduce the necessary specimens and testing duration, possible prediction for the fatigue-limit is conducted with S-N curve. Using a lock-in thermography system, this study examined the distribution of stresses in specimens by applying the principle of thermal elasticity's.

1. Introduction

Infrared thermography is a process to obtain images by using an infrared camera to detect the radiation from an object at an absolute temperature of not less than 0 degree. The portions at a higher temperature are expressed in red, and those at a lower temperature are in blue. The distribution of temperature on the surface of an object can be shown in an image, and the temperature at each portion can be determined [1,2].

Vehicle manufacturers have used FEM and CG for analysis of stress, vibration, and strength, and the verification using fatigue testing is still required. Aircraft or construction machine manufacturers carry out stress tests using strain gauge methods as their specimens are large-sized. If they are able to expect any points on which the stresses are to be concentrated on and which are to be risky, the tests will be much facilitated. With the achievement of sufficient safety and durability, attentions have been shifted to shortening the length of development, lowering the costs, making lighter, and resolving environmental issues. Conventional fatigue testing which requires a long period of time and a lot of costs cannot be a good solution to those concerns Thermography could become used for the estimation of fatigue limits because the noise equivalent temperature difference (NETD) of infrared cameras has been so dramatically enhanced as to develop non-contact and non-destructive inspection technologies for full-field stress analysis [4].

As one of the active infrared thermography measurement methods, a lock-in thermography system consists of an infrared thermography camera, which detects the radiation from the surface of a specimen under periodic loads, and a real-time collector, i.e. lock-in module, which extracts loading signals from a fatigue tester from noises and measures fine variations in temperature [4]. This study used an infrared thermal camera and applies lock-in thermography into the principle of thermoelasticity [5] to monitor the temperature increases of the dispersion energy from the test specimens and accordingly to estimate the stresses and fatigue limits.

[1+] Corresponding author, major of bio-mechanical engineering, KNU, 340-702, Korea : Tel.: +82-41-330-1283, Fax: +8241-330-1283, e-mail: kwt@kongju.ac.kr

2. Theory of Lock-in Thermography

2.1. Thermoelastic stress

Infrared thermographic images are interpreted based on the thermoelastic effect generated by period loads to specimens. The variations in temperature measured by the detector are proportional to the main stresses and are converted to the stresses (MPa) by multiplying the variaton in temperature ($\triangle T$) captured by the infrared camera and the heat elastic modulus (Km). The total sum of the main

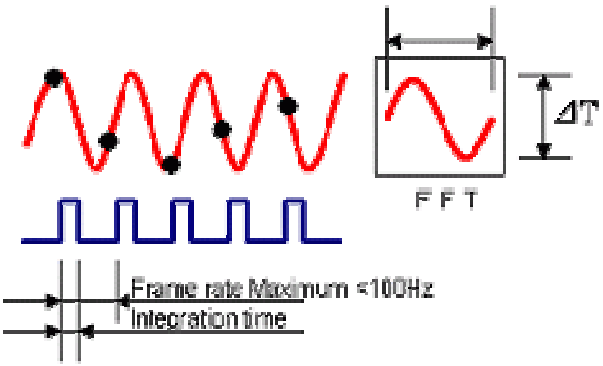

Fig. 1 E-mode processing in Lock-in Thermography

loads on infrared thermography images are obtained by Equation (1)

$$\Delta T = -K_m \cdot T \cdot \Delta\sigma \qquad (1)$$

where,

ΔT : Differences of temperature

K_m : Thermoelastic coefficient,

$\Delta\sigma$: Total summation of major stress

Equation (1) is only applicable when: the adiabatic effect is maintained, i.e. heat generated by the thermoelastic effect is accumulated in a specimen; the heat radiation from the specimen surface is kept in equilibrium; and there is not any external factor, e.g. wind.

In most cases, the adiabatic effect by the thermoelastic effect is greater than the adiabatic effect from the specimen surface, so that the specimen is gradually heated under loads.

2.2. Dissipation energy

In addition to the linear increase or decrease in temperature which is not accompanied by the temperature increase in specimens, consideration should be given to the repetition of temperature increase and decrease by the thermoplastic effect, temperature increase of the dispersion energy by mechanical behaviors in specimens, temperature change by external factors, e.g. wind, and thermal conduction. Equation (2) shows the acual variations in temperature, including the curved increase and decrease in temperature accompanied with the temperature rise in Fig. 1.

$$\Delta T = T_e - T_c + D + T_e \qquad (2)$$

where,

T_e : External sources
(winds or surrounding temperature)

T_c : Heat conduction
(equilibrium status of temperature)

D: Dissipation energy
(temperature rise from repeated cycle)

T_e : Thermoelastic effect

The lock-in thermography only measures the variations in temperature by the thermoelastic effect

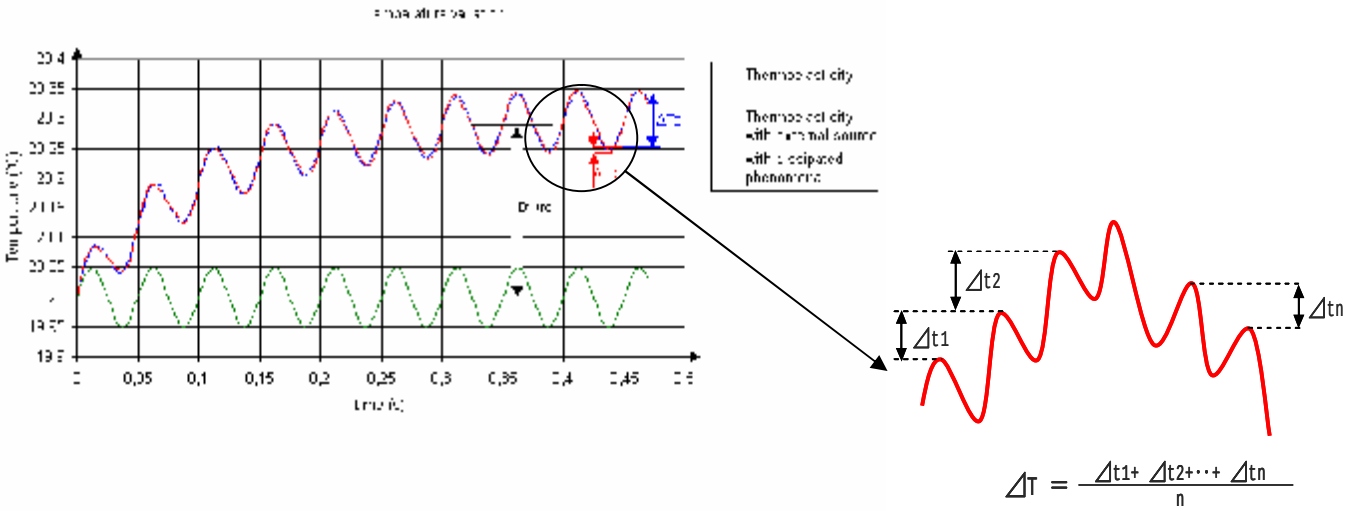

(a) Temperature modulation on loading condition (b) Averaging of ΔT

Fig. 2 Determination of dissipation energy from sinusoidal wave in D-mode

based on synchronized input signals and excludes

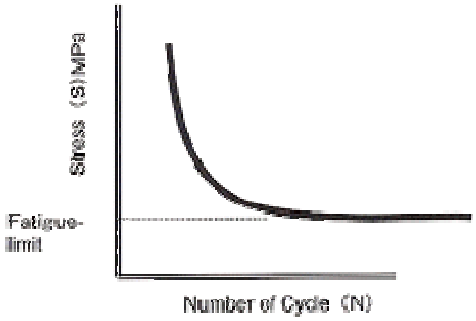

Fig. 3 S-N Curve in Fatigue-limit prediction

the variations in temperature by external factors. If the increases in temperature of the dispersion energy by mechanical behaviors under smaller periodic cycles are separated from the the increment and decrement in temperature by the thermoelastic effect necessary to measure the stresses in the same method as the stress measurement, the thermographic images of the increases in temperature of dispersion energy can be obtained [4].

2.3. Prediction of fatigue-limit

The increase in temperature of the dispersion energy is generated by the internal friction on the specimen surface until its fracture, i.e. hysterisis. On the dispersion energy images, an exothermic portion on which stress is concentrated on is shown. In this portion, greater heat is generated mechanically and dispersion energy is thus greater. Fatigue damages are concentrated on this portion, resulting in fracture. The heating of the dispersion energy depends on the intensity of stresses or loads, shape of specimens, and periodic frequency and incicates the variations in temperature according to mechanical properties.

If loads are applied to a specimen by stages and the increases in temperature of the dispersion energy at each step of load are measured, it is possible to estimate the fatigue limit from the increases in temperature. According to the diagrams with the increases in temperature of the dispersion energy captured by the infrared camera on the longitudinal axis and with the periodic loads applied to the specimen on the horizontal axis, raising the load generates a slow increase in temperature until the fatigue limit, while it creates a faster increase in temperature although it does not result in an immediate fracture.
If drawing a straight lines drawn according to each variation in temperature, there will be two straight lines by the difference in temperature rise rate. The inflection point is located at the same point as the one in the S-N fatigue test curve as shown in Fig. 3 [5].

3. Experiments

3.1. Set-up of experimental apparatus

To measure the thermoelastic stresses and dispersion energy, compact tensile specimens were mounted on MTS 858 Table Top System as shown in Fig. 4. The compact tensile specimen is shown in Fig. 5. The specifications of the specimens are listed in Table 1.

Table 1: Specimen's material type and properties

Material	E, GPa Y module	μ	σ , MPa yield	σ , MPa ultimate
SGC400-1	205	0.3	359	439

The infrared thermographic camera used for this study was Jade 550 M (Cedip, France) with InSb as an infrared detector, temperature range between 5°C to 500°C, resolution of 320x240 pixels (30 µm

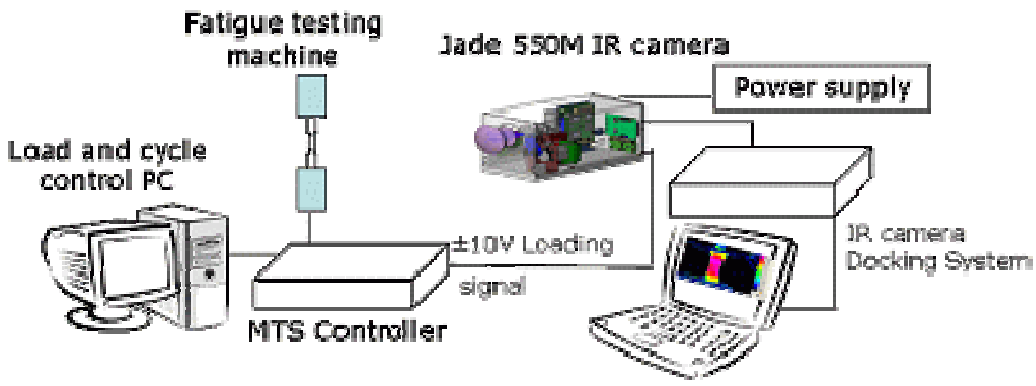

Fig. 4 Schematic diagram of experimental apparatus set-up in Lock-in Thermography

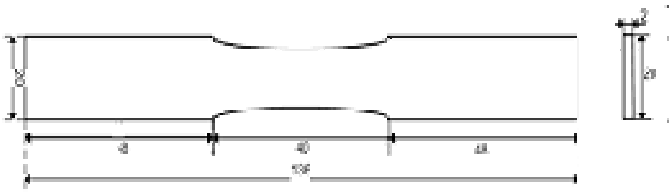

Fig. 5 Schematic diagram of STS; unit mm

pitch), infrared wavelength between 3.6 μm to 5.1 μm, cooling by electronic control of stirling cooler, noise equivalent temperature difference (NETD) of 0.02°C at 25°C, integration time between 1 μs to 10 ms, and frame rate of 170 Hz, i.e. 170 images per second.

3.2. Experimental condition

An infrared (IR) camera was located 0.7 m in front of the specimen, and a lock-in module which synchronizes in real time the loading signals of the fatigue tester and the temperature data from the camera as shown in Fig. 4. The IR camera had a frame setting speed of 70 Hz, and the ambient temperature was 25°C. The specimen was covered with dull and black paints with a radiation rate of ε 1.0. Table 2 shows the engineering data for materials, including the specimen.

Table 2: Typical engineering values form common materials

Material	α K^{-1}	ρ Kgm^{-3}	Cp	Km MPa^{-1}
Steel	1.20e-5	7800	490	3.14e-6
Cast iron	1.00e-5	7800	500	2.56e-5
Iron	1.21e-5	7870	441	3.49e-6
Aluminum	7.70e-5	3900	990	1.99e-6

The MTS fatigue tester had a loading frequency of 15 Hz. All the heating elements were removed from the laboratory room to make the test conditions as close to adiabatic conditions as possible.

3.3. Experimental procedure

Specimens were mounted on the MTS fatigue tester, and two journals of specimen were fastened. Tensile loads were applied from 100 MPa to 400 MPa by stages with increment of 50 MPa. In this study, experimental process are as follows; (1) The thermographic camera was set to the frame rate of 70 Hz, and the MTS fatigue tester was set to a loading frequency of 15 Hz and load of 100 MPa. When the load reach 25 MPa, fatigue loads of 0-50 MPa (±25 MPa) were applied. When the load reached 50 MPa, fatigue loads of 0-100 MPa (±25 MPa) were applied. (2) At the point of 200 cycles, about 4,000 images were recorded at the E-mode. (3) At the point of 3,500 cycles, about 4,200 images were recorded at the D-mode for 60 seconds. (4) After the recording, the procedures (2) and (3) were repeated at each load of 150, 200, 250, 300, 350, and 400 MPa.

4. Results and Discussions

4.1. External load and thermoelasticity

The infrared stress images and the temperature increases by dispersion energy were obtained and measured at each load using the IR camera. Fig. 7 shows the stresses (MPa) converted from the infrared stress images by multiplying the temperature increases of the thermoelastic effect (Te) by the periodic loading to the specimen in Equation (1) and the heat elastic modulus of the specimen.[6,8] Graphing the maximum stresses at the corners of the specimens on which stresses are concentrated in the infrared stress images in Fig. 6

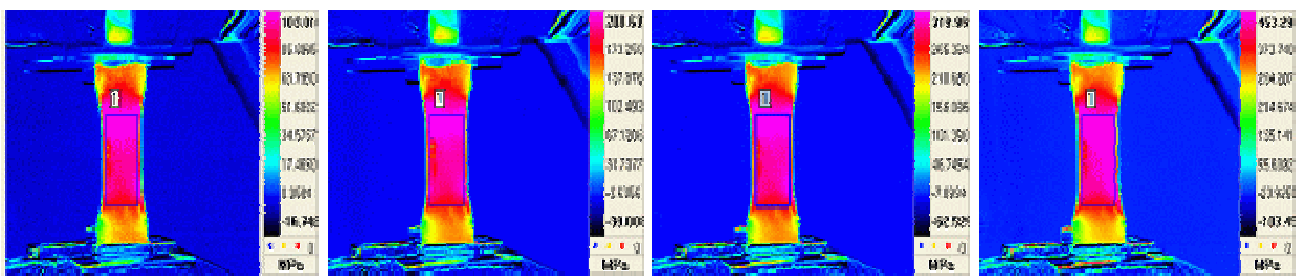

(a) 100 MPa (b) 200 MPa (c) 300 MPa (d) 400 MPa

Fig. 6 Thermographies of stress distribution on STS

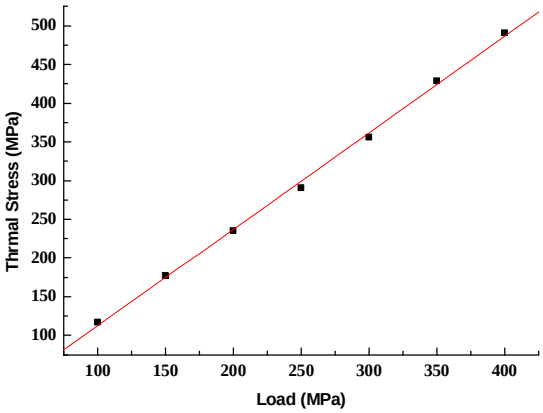

Fig. 7 Relationship between stress and loading

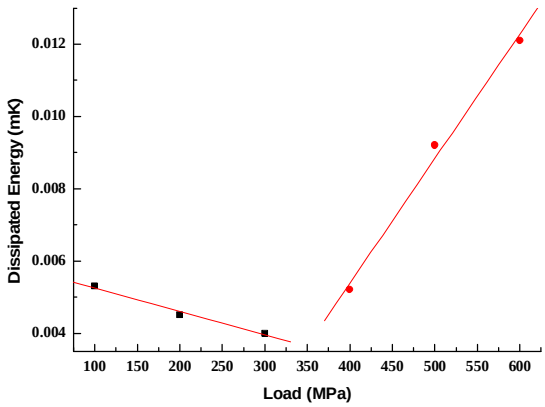

Fig. 8 Fatigue-limit prediction according to dissipation energy

indicated that the stresses (MPa) which the IR camera captured for the filtered loads are in proportion to the loads as shown in Fig. 7. This proves that the variations in temperature captured by the IR camera are equal to the loads actually applied to the specimens.

4.2. Dissipation energy and fatigue-limit

In Fig. 8, the inflection point of the two lines wth different increases in temperature caused by the internal friction, i.e hysterisis, corresponds to the fatigue limit as described above. Fig. 9 shows the maximum temperatures from the dispersion energy images at the specimen corners on which loads were concentrated. The dispersion energy images show the temperature increases, △T (°C), in Equation (5).[9]

From Fig. 8, the load corresponding to the fatigue limit of the test specimen was about 300 MPa. It took about 2~3 minutes to obtain each image, and it only took about 3 hours to carry out the estimation the fatigue limit including the preparation. In steel, it would take 10^7 cycles to obtain the same result in

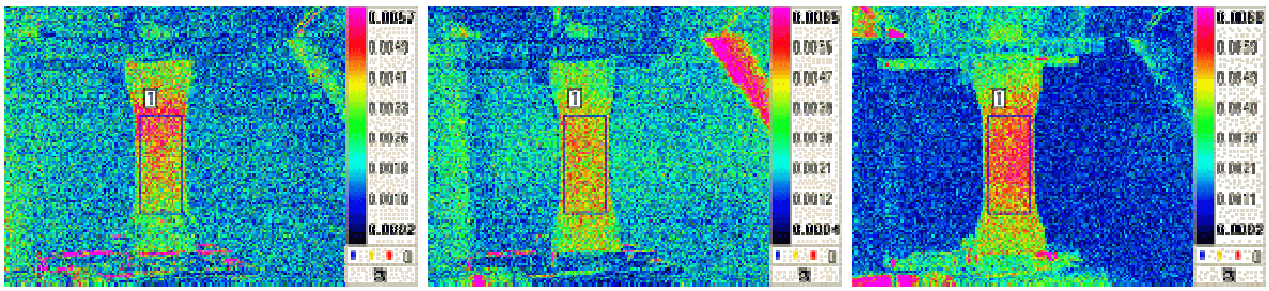

(a) 100 MPa (b) 150 MPa (c) 200 MPa

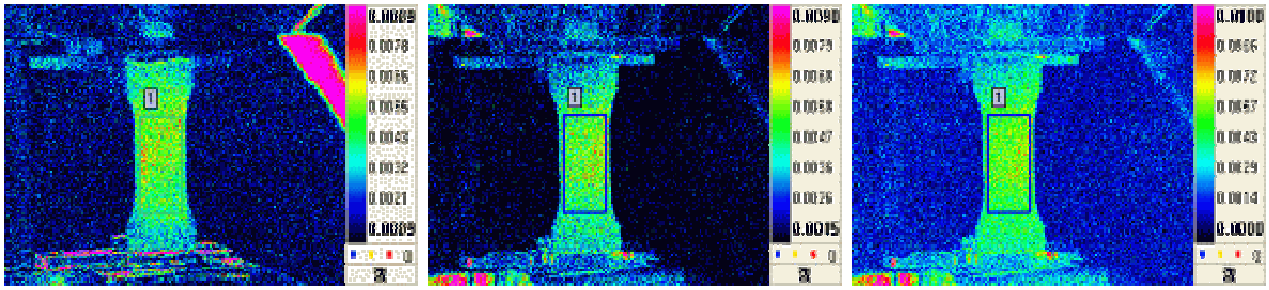

(a) 250 MPa (b) 300 MPa (c) 350 MPa

Fig. 9 Thermographies of dissipation energy on STS

conventional fatigue tests.

5. Conclusions

This study analyzed the stress images, which were created by the thermoelastic effect under the periodic loads to specimens and detected by the infrared thermography camera, to estimate the fatigue limit from the relationship between the loads applied and the dispersion energy. It was shown that the thermography was a effective method to estimate fatigue limits in a shorter period of time in fatigue testing without fracture of specimens.

Although this technology cannot be applied to all fatigue testing, the combination of infrared thermography and fatigue testing will help reduce the number of prototypes and specimens to be fractured and the period of time taken for fatigue tests.

6. References

[1] Vavilov V., *Thermal nondestructive testing: short history and state-of-art. In: Balageas D, Busse G, Carlomagno GM,* editors Proceedings of the QIRT92, Eurotherm Series 27. EETI ed., p.179-93, 1992.

[2] Won T. Kim, Man Y. Choi, Jung H. Park, "Diagnosis of defect points in materials using infrared thermography," *Key Engineering Materials, Vols*. 297~300, p. 2169~2173, 2005.

[3] Pierre Bremond and Pierre Potet, *Cedip Inferared Systems : Lock-in Thermography, A tool to analyze and locate thermo-mechanical mechnism in materials and structure.*, Thermosence XXIII April 2001.

[4] Minh P. L., *Fatigue limit evaluation of metals using an infrared thermographic technique., Mechanics of materials* 28, p. 155-163, 1998.

[5] Pierre Bremond and Pierre Potet, *Cedip Inferared Systems , Lock-in Thermography, A tool to analyze and locate thermo-mechanical mechnism in materials and structure., Thermosence* XXIII April 2001.

[6] Jung H. Park, Man Y. Choi, Won T Kim, "Infrared thermography and modeling to the concrete deck with internal defects as a non-destructive testing," *Key Engineering Materials, Vols*. 270~273, p. 938~943, 2004.

[7] Avdelidis, N.P., Hawtin, B.C., and D.P. Almond, "Transient thermography in the assessment of defects of aircraft composites", *J. NDT& E Int.*, 36:433–439, 2003.

[8] Bates, D., Smith, G., Lu, D. and Hewitt, J., "Rapid thermal nondestructive testing of aircraft components," *J. of Compos. Part B: Eng.*, 31:175–85, 2000.

[9] Vavilov, V.P. and Taylor, R. *Research techniques in NDT, R. Sharpe editor*, England, Academic Press, London, 1982.